Hydrothermal Liquefaction of a Microalga with Heterogeneous Catalysts

ARTICLE *in* INDUSTRIAL & ENGINEERING CHEMISTRY RESEARCH · JANUARY 2011

Impact Factor: 2.59 · DOI: 10.1021/ie100758s

2 AUTHORS:

Peigao Duan
Henan Polytechnic University
44 PUBLICATIONS **961** CITATIONS
SEE PROFILE

Phillip E. Savage
University of Michigan
197 PUBLICATIONS **7,586** CITATIONS
SEE PROFILE

Hydrothermal Liquefaction of a Microalga with Heterogeneous Catalysts

Peigao Duan and Phillip E. Savage*

Chemical Engineering Department, University of Michigan, Ann Arbor, Michigan, 48109-2136

We produced crude bio-oils from the microalga *Nannochloropsis sp.* via reactions in liquid water at 350 °C in the presence of six different heterogeneous catalysts (Pd/C, Pt/C, Ru/C, Ni/SiO_2−Al_2O_3, CoMo/γ-Al_2O_3 (sulfided), and zeolite) under inert (helium) and high-pressure reducing (hydrogen) conditions. To our knowledge, this is the first application of common hydrocarbon processing catalysts to microalgae liquefaction in water. In the absence of added H_2, all of the catalysts tested produced higher yields of crude bio-oil from the liquefaction of *Nannochloropsis sp*., but the elemental compositions and heating values of the crude oil (about 38 MJ/kg) were largely insensitive to the catalyst used. The gaseous products were mainly H_2, CO_2, and CH_4, with lesser amounts of C_2H_4 and C_2H_6. The Ru and Ni catalysts produced the highest methane yields. Only the zeolite catalyst produced significant amounts of N_2. Typical H/C and O/C atomic ratios for the crude bio-oil are 1.7 and 0.09, respectively. In the presence of high-pressure H_2, the crude bio-oil yield and heating value were largely insensitive to the presence or identity of the catalyst. The presence of either the hydrogen or the higher pressure in the reaction system did suppress the formation of gas, however. The total gas yield was always lower in H_2 than it was in analogous experiments without H_2 and at lower pressure. In both the presence and absence of H_2, the supported Ni catalyst produced a crude bio-oil with a sulfur content below the detection limits. This apparent desulfurization activity for the Ni catalyst was unique to this material.

1. Introduction

Biofuel can be broadly defined as solid, liquid, or gaseous material consisting of or derived from a renewable biomass resource. The use of edible biomass (e.g., corn, soybeans) for production of first-generation liquid biofuels (grain ethanol, soy biodiesel) has been the subject of much debate, as it can lead to fuel vs food competition. In contrast, second-generation biofuels arise from nonfood feedstocks such as lignocellulosic biomass and jatropha oil, yet the end product remains the same as in the first generation (e.g., ethanol, biodiesel). Third generation biofuels, though still from nonfood feedstocks, are fungible and thus drop-in replacements for their petroleum counterparts.

Microalgae are an especially promising feedstock for advanced biofuels because of their higher photosynthetic efficiency, faster growth rate, and higher area-specific yield relative to terrestrial biomass. Microalgae can be cultivated in saline/brackish water and on nonarable land so there is no competition with conventional crop land. Further, microalgae have the ability to accumulate large amounts of lipids. Water needs for microalgae, however, and some environmental impacts may exceed those of selected terrestrial crops.[1]

Conventional thermochemical methods for fuel production from biomass (e.g., gasification, fast pyrolysis) require a dry feedstock or they will suffer a large energy penalty from vaporizing the moisture content. Many potential feedstocks, and especially microalgae, however, have very high moisture contents. Therefore, aqueous-phase processing of such biomass feedstocks is attractive from an energy perspective. Hydrothermal gasification and hydrothermal liquefaction are being explored for the aqueous-phase conversion of wet biomass into biofuels.[2−6]

Hydrothermal liquefaction converts biomass into an oily or tarry fluid via reactions in and with liquid water at elevated temperatures (200−350 °C), where water can serve as solvent, catalyst (or catalyst precursor), and reactant (e.g., in hydrolysis reactions).[7] This high-temperature liquid water (HTW) exhibits properties that are very different from those of liquid water at room temperature. It has a lower dielectric constant, fewer and weaker hydrogen bonds, a higher native H^+ concentration (which facilitates acid-catalyzed reactions), and a higher solubility for small organic compounds.[8]

There has been some previous work that examined microalgae as a feedstock for hydrothermal liquefaction. Most of these previous studies, however, involved uncatalyzed liquefaction. When catalysts have been used, they were typically water-soluble inorganic compounds such as Na_2CO_3 or KOH.[9−13] Previous studies on the hydrothermal liquefaction of microalgae in the presence of potential heterogeneous catalysts are rare. To our knowledge, only Jena and Das[14] have entered this arena. These investigators used NiO to assist in the liquefaction of both a single (*Spirulina*) and mixed algae (from open ponds with wastewater) at 350 °C. Interestingly, the added NiO decreased oil yields but led to a higher fraction of C in the gaseous products. Ni is known to be a good hydrothermal gasification catalyst.[5] Indeed, catalytic hydrothermal gasification to CH_4 has been demonstrated for many different types of biomass.[5]

To our knowledge, the Jena and Das study is the only previous examination of microalgae liquefaction in HTW in the presence of a potential solid catalyst. There has been no previous study of solid catalysts commonly used to refine petroleum crude oil and produce transportation fuels. Furthermore, though there has been catalyst screening work done for hydrothermal gasification,[15−17] there has been no previous study wherein a range of catalysts was used to liquefy the same microalga feedstock at identical conditions.

The objective of the present work is to determine the influence of several different, but common, heterogeneous catalysts on the bio-oil and gaseous products from hydrothermal liquefaction of a representative microalga. We selected *Nannochloropsis sp.*, a marine microalga. These experiments used three noble metal

* Corresponding author. E-mail: psavage@umich.edu.

10.1021/ie100758s
Published on Web 08/16/2010

Table 1. Analysis of *Nannochloropsis sp.*

property	value
moisture content (wt %)	78%
ash content (wt %, dry basis)	18%
chemical composition (wt %, per supplier)	
crude protein	52%
carbohydrates	12%
lipids	28%

Table 2. Catalyst Compositions

catalyst	composition (from supplier)
Pd/C	Pd (5 wt %)
Pt/C	Pt (5 wt %)
Ru/C	Ru (5 wt %)
$Ni/SiO_2-Al_2O_3$	Ni (65 wt %)
$CoMo/\gamma\text{-}Al_2O_3$	CoO (4.4 wt %), Mo_2O_3 (11.9 wt %), sulfided
zeolite	SiO_2 and Al_2O_3, in various proportions plus metal oxides

catalysts supported on carbon (Pd/C, Pt/C, and Ru/C), one typical hydrotreatment catalyst (sulfided $CoMo/\gamma\text{-}Al_2O_3$), one transition metal catalyst supported on silica−alumina ($Ni/SiO_2-Al_2O_3$), and one zeolite (aluminum silicate) catalyst. The noble-metal catalysts (Pd, Pt, Ru) were selected on the basis of their high activity toward the reduction of a wide range of different oxygenates to hydrocarbons. Thus, these catalysts might be effective for hydrogenation reactions and oxygen removal from the bio-oil. Ni was selected because it is used as a hydrogenation catalyst. Sulfided CoMo catalysts are commonly used to remove heteroatoms from petroleum crude oil, so this material might be effective for removing O, N, and S from the biocrude. Zeolite was tested because aluminosilicates can facilitate cracking reactions that will convert the heavier components of the biocrude into smaller fuel-range molecules. Some of the catalysts we used lack long-term stability in a hydrothermal environment because they are susceptible to sintering (e.g., Ni), dissolution (e.g., SiO_2), or phase transitions (e.g., $\gamma\text{-}Al_2O_3$).[17,18] We did not disqualify any of the catalysts from consideration because of this process-related issue. Rather, we chose to be inclusive with the catalysts since our goal was to learn whether these materials would be effective in short-term liquefaction experiments. If a material that lacks long-term stability shows promising short-term effects, then additional work can be done to develop different formulations that are both active and stable.

2. Experimental Section

2.1. Materials. Microalga (*Nannochloropsis sp.*) paste was purchased from Reed Mariculture (Nannochloropsis 3600). Table 1 lists its properties. All but one of the catalysts were obtained from Sigma-Aldrich. $CoMo/\gamma\text{-}Al_2O_3$ (sulfided) was obtained from Alfa Aesar. Table 2 gives the supplier-provided nominal compositions for each catalyst. All catalysts were used as received. Freshly deionized water, prepared in house, was used throughout the experiments. All other chemicals were purchased from Fisher Scientific in high purity and used as received. Helium, hydrogen, and argon were obtained from Cryogenic Gases. Gas standards for instrument calibration were purchased from Air Liquide Specialty Gases.

We used 316-stainless steel reactors that allowed for the recovery and analysis of both the liquid- and gas-phase products in a single run. The reactors, illustrated in Figure 1, had a volume of 31 mL and consisted of an 8 in. length of $^3/_4$ in. O.D. tube with a wall thickness of 0.065 in. A cap was placed on one end, and the other end was fitted with an 8.8 in. length of $^1/_4$ in. O.D. tube, with a wall thickness of 0.035 in., connected to an HiP high-pressure valve.

Figure 1. Batch stainless steel reactor.

2.2. Procedure. Prior to their use in experiments, the reactors were loaded with water and seasoned at 350 °C for 60 min to remove any residual organic material from the reactors and to expose the fresh metal walls to HTW. The reactors were then gradually cooled to ambient temperature and thoroughly washed with acetone and air-dried. We also pressure tested the assembled reactors with helium prior to use.

In a typical experiment, 0.384 g catalyst was loaded into the reactor. This amount represents a 50 wt % loading with respect to dry microalgae on an ash-free basis. Microalgae paste (4.27 g) was loaded next, and then 13.5 mL of freshly deionized water was added. The water loading was selected such that 95% of the reactor volume would be occupied by liquid at reaction conditions, if water were the sole component. After the reactors were loaded, the cap assembly was connected and securely tightened to seal the reactor. The air inside the reactor was displaced with helium by repeated cycles of evacuation and charging with He (70 kPa, gauge). The 70 kPa of helium that remained served as an internal standard for the quantification of gas yields. In some experiments, the reactor was further charged with hydrogen at this point to 3500 kPa. After pressurization with He (and at times H_2), the reactor valve was securely tightened and the reactor assembly then disconnected from the gas manifold.

Reactions were carried out by placing the reactors vertically in a Techne Fluidized Sand Bath (model SBL-2), and the temperature was maintained at 350 °C by a Techne TC-8D temperature controller with a precision of ±2 °C. Heat up time was about 3 min, and the total batch holding time was 60 min. The reactors were removed from the sand bath and immersed in a cold-water bath for about 5 min to quench the reaction. The reactors were further cooled in a refrigerator for 30 min. The reactors were then removed from the refrigerator and placed in ambient conditions for at least 15 h to allow the liquid and gas phases to equilibrate. Three or four independent runs were conducted under nominally identical conditions to determine the uncertainties in the experimental results. Results reported herein represent the mean values for the independent trials. Uncertainties are reported as the experimentally determined standard deviations.

2.3. Gas-Phase Analysis. The gas phase was analyzed with an Agilent Technologies model 6890N gas chromatograph (GC) equipped with a thermal conductivity detector (TCD). A 15 ft × $^1/_8$ in. i.d. stainless steel column, packed with 60 × 80 mesh Carboxen 1000 (Supleco) separated each component in the mixture. Argon (15 mL min^{-1}) served as the carrier gas for the analysis.

The reactor was connected to the GC gas sampling valve, and the gases in the reactor flowed into the sample loop as the reactor valve was opened slowly and slightly to allow about a 1 mL sample to exit. The gas sample was sent to the column via a Valco switching valve, which was automated with an air actuator. After the switching valve closed, the reactor valve was also closed. To ensure that the GC sample is representative of the gas mixture in the reactor, a subsequent analysis was conducted. Thus, two consecutive analyses of the gas mixture were taken for each reactor. The temperature of the column was

initially held at 35 °C for 5 min and then it increased to 225 °C at a rate of 20 °C min^{-1}. The final temperature was held for 15 min.

The mole fraction of each gaseous component was determined via calibration curves generated from analysis of the analytical gas standards with known composition. The amount of helium added to the reactor was used as an internal standard to determine the molar amount of each constituent. The yield of each gas species was calculated as its molar amount divided by the mass of dry microalgae loaded into the reactor.

2.4. Crude Bio-oil Analysis. After analyzing the gas fraction, we opened the reactors to recover the liquid fraction. Approximately 10 mL of dichloromethane was added, and the reactor was capped and shaken vigorously by hand. The reactor contents, including catalyst, were then transferred to a glass separatory funnel. The reactor was washed twice more with additional 10 mL aliquots of dichloromethane to ensure that all the contents were collected and transferred to the separatory funnel. The separatory funnel was then shaken to mix its contents. When the organic and aqueous phases had separated, the heavier phase (containing catalyst and organics) was withdrawn and retained for catalyst separation. The upper aqueous phase was then extracted with sequential 20 and 10 mL aliquots of dichloromethane. All of the dichloromethane extracts were combined, and the catalyst was recovered by filtering the solution. All of the filtrate was carefully transferred to a round-bottom flask, and the solvent was evaporated under a vacuum of 27 kPa at 30 °C for 5 min. The flask was then quickly capped and weighed to determine the mass it contained. The material remaining in the flask is the crude bio-oil plus some residual dichloromethane. To estimate this residual solvent amount, we performed a control experiment wherein we treated a flask containing pure dichloromethane alone to this evaporation procedure. The mass of residual solvent (0.17 g) in the control experiment was subtracted from the sample masses to estimate the mass of the crude bio-oil produced in each experiment. The crude bio-oil yield was calculated as its mass divided by the mass of dry microalgae loaded into the reactor. Since the amount of residual solvent in each biocrude sample is estimated as described above, the biocrude yields we report are necessarily approximate and subject to systematic error. Nevertheless, we expect the trends in the yields, which should be largely insensitive to any systematic error, to be reliable.

An Agilent Technologies 6890N GC equipped with an autosampler, autoinjector and mass spectrometric detector was used to analyze the bio-oil (redissolved in dichloromethane). An Agilent J&W DB-5HT nonpolar capillary column (30 m length, 0.25 mm i.d., 0.10 μm film thickness) separated the constituents. A volume of 2 μL was injected for each sample, and the inlet split ratio was 5:1. The column was initially held at 80 °C for 2 min. The temperature was ramped to 300 at 3 °C min^{-1} and held isothermally for 10 min, giving a total runtime of about 85 min. Helium served as the carrier gas (20 mL min^{-1}). A Wiley mass spectral library was used for compound identification.

^{1}H NMR and ^{13}C NMR spectra of crude bio-oil were recorded at 400.0 and 100.6 MHz, respectively, on a 400 MHz NMR spectrometer (Inova 400, Varian) at a temperature of 25 °C. The bio-oil sample (8 wt %) was dissolved in $CDCl_3$. About 10^5 scans were accumulated for the ^{13}C spectrum using a 45° pulse width together with broad band proton decoupling. NMR tubes of 5 mm diameter were used.

Fourier transform infrared spectroscopic analysis (FT-IR) was performed on a Nicolet 6700 FT-IR spectrometer (Thermo Electron Corp.) to determine the functional groups in the crude bio-oil. FT-IR spectra (resolution: 4 cm^{-1}, scan: 254, range: 4000−400 cm^{-1}) were taken after spreading a thin film of sample on a multibounce plate of ZnSe crystal at a controlled ambient temperature (25 °C). A background spectrum was also collected under identical conditions.

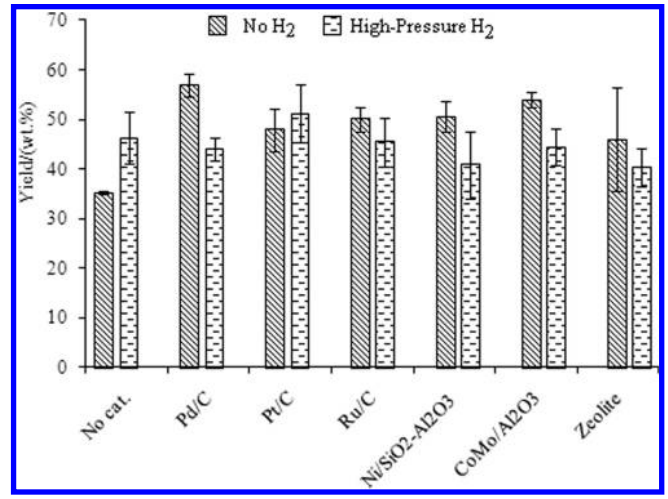

Figure 2. Yields of crude bio-oil from liquefaction with different catalysts and reaction environments.

The elemental compositions (C, H, O, N, and S) of the microalga and the biocrude were determined by Atlantic Microlab, Inc. All residual dichloromethane was evaporated prior to elemental analysis. The higher heating values of the biocrude and dry microalga were estimated by using the Dulong formula

$$\text{heating value (MJ/kg)} = 0.338C + 1.428(H - O/8) + 0.095S$$

where C, H, O, and S are the wt % composition of each element in the organic material.

3. Results and Discussion

This section provides information about the biocrude and gas products formed during hydrothermal liquefaction in the presence and absence of the different catalysts. We first discuss the influence of the different catalysts on the oil yields and composition, and then provide a detailed molecular characterization of one of the biocrudes from catalytic liquefaction. The final sections present results from the gas-phase analysis and from overall mass and energy balances for the liquefaction feedstock and products.

3.1. Effect of Catalysts on Oil Yields. Figure 2 shows the effects of various catalysts on the crude bio-oil yield obtained from the liquefaction of *Nannochloropsis sp.* with and without high-pressure hydrogen. The crude bio-oil yields range from a low of 35% from uncatalyzed liquefaction without H_2 to a high of 57% from Pd/C catalyzed liquefaction without H_2. This 35% yield from uncatalyzed liquefaction is lower than the yield of 43% that we reported in an earlier article.[19] The only differences in the experiments were using a different shipment of microalgae, a higher algal biomass loading in the reactor (0.031 g/cm^3 vs 0.028 g/cm^3 used previously), and less of a vacuum when the dichloromethane solvent was evaporated. We cannot state with certainty that these factors alone caused the difference in yields. It is possible that the difference could simply be due to experimental variability.

Table 3. Elemental Composition, Atomic Ratios, and Heating Value of Bio-Crudes (No Added H_2)

	dry algae	no cat.	Pd/C	Pt/C	Ru/C	$Ni/SiO_2-Al_2O_3$	$CoMo/Al_2O_3$	zeolite
C (wt %)	43.0	75.3	73.4	75.9	72.6	75.0	75.7	69.6
H (wt %)	5.97	10.2	10.8	10.8	10.3	10.2	10.3	9.44
O (wt %)	25.8	9.18	9.01	8.48	9.34	8.59	8.50	9.46
N (wt %)	6.32	4.18	3.88	4.04	3.49	3.74	4.31	4.33
S (wt %)	0.58	0.84	0.52	0.72	0.31		0.58	0.74
H/C	1.67	1.63	1.76	1.71	1.70	1.62	1.63	1.63
O/C	0.45	0.091	0.092	0.084	0.097	0.086	0.084	0.100
HHV (MJ/kg)	18.5	38.5	38.6	39.6	37.5	38.3	38.8	35.4

Table 4. Elemental Composition, Atomic Ratios, and Heating Value of Bio-Crudes (3500 kPa H_2)

	dry algae	no cat.	Pd/C	Pt/C	Ru/C	$Ni/SiO_2Al_2O_3$	$CoMo/Al_2O_3$	zeolite
C (wt %)	43.0	75.5	74.9	76.1	73.2	76.2	74.8	74.2
H (wt %)	5.97	10.5	10.6	11.1	10.6	10.7	10.4	10.5
O (wt %)	25.8	9.23	9.04	8.34	8.63	9.01	8.55	8.92
N (wt %)	6.32	4.08	4.20	3.92	3.33	3.64	3.99	4.05
S (wt %)	0.58	0.69	0.65	0.62	0.42		0.56	0.88
H/C	1.67	1.68	1.70	1.74	1.74	1.68	1.66	1.69
O/C	0.45	0.092	0.090	0.082	0.088	0.089	0.086	0.090
HHV (MJ/kg)	18.5	39.0	38.9	40.1	38.4	39.4	38.6	38.5

Note that all of the crude bio-oil yields reported here exceed the crude lipid content (28 wt %) of the feedstock. This result, which has also been observed in previous microalgae liquefaction studies, shows that not only the triglycerides but also other cellular components such as protein, fiber, and carbohydrate, must be converted into crude bio-oil. This ability to convert different biomacromolecules into a biocrude suggests that hydrothermal liquefaction could be widely applied to various microalgae and other wet biomass resources.

Figure 2 shows that the addition of catalysts promoted production of crude bio-oil during liquefaction in an inert environment. With the exception of the high yield from Pd/C, the yields from all of the other catalysts were essentially the same as (about 45−50%) but higher than the yield from uncatalyzed liquefaction. This similarity in yields is interesting since the catalysts were all quite different. As shown in Table 2, they had different metals, different metal loadings, and different supports, which likely had different surface areas and different pore size distributions. The yields from zeolite-catalyzed liquefaction show the greatest run-to-run variability. The most likely reason for this larger uncertainty is the difficulty we had in recovering all of the "oil" in these experiments, due to its very high viscosity and tarry nature.

Though the oil yield from liquefaction without H_2 was not highly sensitive to the catalyst identity, the color and apparent viscosity of the crude bio-oil did vary depending on the catalyst type. For example, the crude bio-oils obtained with Pd/C, Pt/C, Ru/C, and CoMo/γ-Al_2O_3 flowed easily and were much less viscous than the oil from uncatalyzed or zeolite-catalyzed liquefaction. The bio-oil produced with the $Ni/SiO_2-Al_2O_3$ catalyst had a dark red color.

Figure 2 shows that the addition of high-pressure H_2 to the reactor led to a higher bio-oil yield from the uncatalyzed liquefaction. Interestingly, it did not have that effect on any of the catalyzed liquefaction experiments. That is, the addition of H_2 did not increase the oil yields from catalyzed liquefaction. The oil yields from hydrothermal liquefaction with added H_2 were all about the same (given their standard deviations), regardless of the catalyst identity or its presence or absence. In fact, for several catalysts, the mean biocrude yield was lower than it was for the noncatalytic liquefaction case. Catalytic hydrothermal gasification reactions could have caused this reduced oil yield. A subsequent section provides results for the gas yields and compositions from these experiments. It is important to note at this point that conditions producing a lower bio-oil yield could be desirable if they also produced a biocrude of higher quality (e.g., if catalytic liquefaction were to produce a lower yield of bio-oil because it had a lower oxygen content but higher heating value). Moreover, if the catalysts promoted hydrocracking reactions wherein large molecules were converted to smaller, more volatile ones, then one could anticipate lower oil yields because more of these lighter molecules would have been lost during the solvent evaporation stage of bio-oil recovery.

One reason for the catalysts having little effect on the oil yields during liquefaction in the reducing environment could be that the oil yield in the absence of catalyst was already near the upper bound of what is possible given the constraint of a simple mass balance. As we will show later in this article, the biocrude produced in the reducing environment with no added catalyst already contained more than 80% of the C and H atoms in the alga feedstock. Therefore, the added catalysts may not have had much of a genuine opportunity to increase the oil yields any further. Of course, other potential explanations (e.g., rapid catalyst deactivation, strong intraparticle diffusion limitations, insufficient metal loadings in the reactor) exist for the absence of a significant influence of the different catalysts on the oil yield. Rapid catalyst deactivation, for example, could occur by the sulfur molecules in the algal biomass. Such sulfur poisoning has been observed in hydrothermal gasification studies.[20] As we will discuss more fully later, we do not believe this poisoning is significant in the present study.

3.2. Effect of Catalysts on Oil Composition. Tables 3 and 4 list the elemental compositions and estimated higher heating values of the crude bio-oil from microalga liquefaction with and without added H_2 in the presence and absence of the different catalysts. The carbon and hydrogen content of the biocrude was always much higher than that of the biomass feedstock, whereas the oxygen content in the oil was reduced to 8.3−9.6 wt % (vs 26 wt % in the feedstock). Of course, the increased C and H levels and reduced O content lead to the crude bio-oil obtained from liquefaction having a much higher energy density than the dry microalga feedstock. The heating values are around 38−40 MJ/kg, which exceed those of crude bio-oils obtained from pyrolysis of microalgae[21] and are very close to those of petroleum-derived fuels (~42 MJ/kg). The oxygen content in the crude algal bio-oil is also much lower than that of bio-oils from pyrolysis of terrestrial biomass.[22]

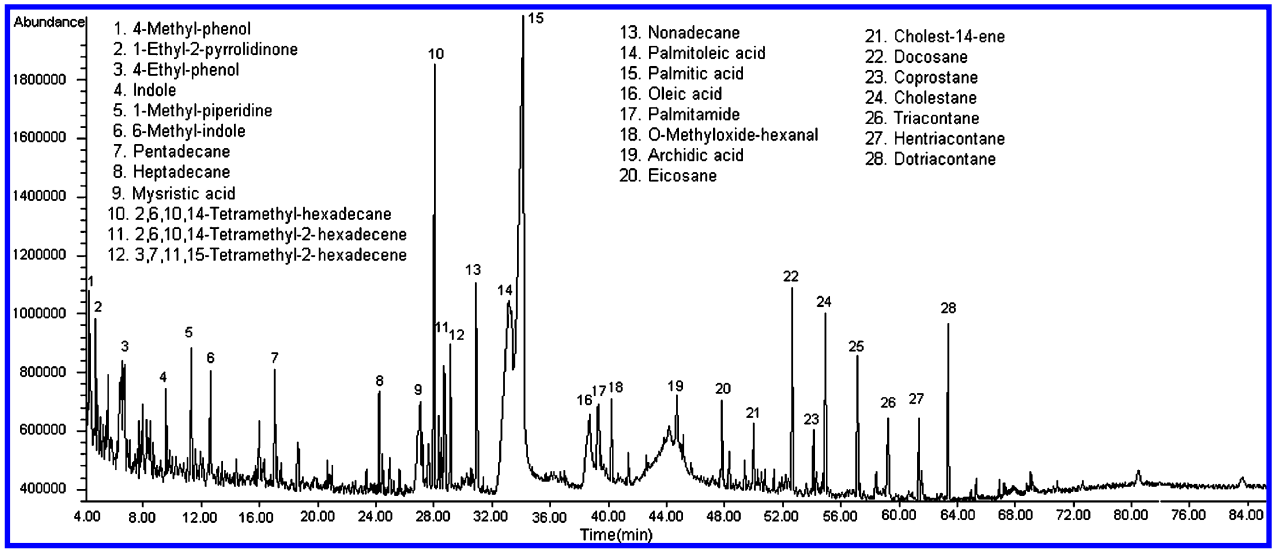

Figure 3. Total ion chromatogram of biocrude (Pd/C, no H_2 added).

Hydrothermal liquefaction alone (no added catalyst) produces a bio-oil with a higher heating value and lower oxygen content than the algal biomass feedstock. Using supported noble metal catalysts (Pt, Pd, Ru), even in the absence of added H_2, increases the H/C molar ratios even further. The presence of Pt, Ni, and CoMo catalysts lead to bio-oils with lower O/C ratios than the oil produced in their absence. These findings indicate that catalytic deoxygenation or hydrodeoxygenation proceeded during the hydrothermal liquefaction of the microalga. Thus, there may be opportunities for a single-step catalytic liquefaction process to produce a higher quality bio-oil than would uncatalyzed liquefaction.

In all but one case (Pd/C), the crude bio-oil obtained under the hydrogen environment had a higher hydrogen content and higher H/C ratio than that produced in the absence of added H_2 at otherwise identical conditions. This increase in hydrogen content was small, however. The biocrude from processing in H_2 also generally had a higher heating value than did the biocrude formed in the inert environment with the same catalyst. Again, this difference is small.

Microalgae usually contain a high proportion of nitrogen due to its presence in chlorophyll and in protein. For the microalga in our experiments, the nitrogen content is 6.3 wt % on a dry basis. Hydrothermal liquefaction leads to a bio-oil with a lower proportion of nitrogen than the starting feedstock. Of the catalysts tested, Ru/C and $Ni/SiO_2-Al_2O_3$ produced oils with the lowest N wt %, both in the presence and in the absence of added H_2. The addition of H_2 led to a lower N wt % for all cases except liquefaction with added Pd/C. The results in Tables 3 and 4 indicate that Ru/C and $Ni/SiO_2-Al_2O_3$ are capable of providing in situ denitrogenation during liquefaction of the microalgal feedstock, and that liquefaction in a H_2 environment removes even more of the original nitrogen atoms.

Ru/C and $CoMo/Al_2O_3$ show some activity for sulfur removal from the microalgal fragments in the bio-oil, but the supported Ni catalyst showed even greater activity. The bio-oils produced by catalytic liquefaction in the presence of $Ni/SiO_2-Al_2O_3$ contained no detectable sulfur. This catalyst seemingly provides complete desulfurization of the bio-oil. This catalyst also had a much higher metal loading (65 wt %) than the others tested, so this difference might explain its relative superiority for removing sulfur. Of course, this desulfurization might be due to adsorption rather than catalytic reaction. Finally, note that in all of these results for the different catalysts, we cannot eliminate the possibility of the supports being responsible for some of the observed effects. Carbon, for example, is known to have modest activity for removing oxygen atoms from fatty acids.[23]

3.3. Molecular Characterization of Crude Bio-oil. In a previous article[19] we provided a molecular characterization of the biocrude produced from uncatalyzed liquefaction of *Nannochloropsis sp.* under an inert environment. In this article we provide some molecular details about the biocrude produced from liquefaction with the Pd/C catalyst. This section presents the first such characterization for an algal biocrude from a heterogeneously catalyzed hydrothermal liquefaction process.

3.3.1. GC−MS Analysis. We used GC−MS to separate and identify several of the molecular components in the crude bio-oil from Pd/C-catalyzed liquefaction in an inert environment. Figure 3 presents a representative total ion chromatogram for the bio-oil dissolved in dichloromethane, and it contains more than 100 peaks. A mass spectral library and computer matching were used to facilitate compound identification. Figure 3 shows the tentative identities of the major (peak area at least 0.5% of the total) individual molecular components in the bio-oil.

The crude bio-oil contains large quantities of fatty acids (peaks 9, 14, 15, 16, and 19), some phenolic compounds (peaks 1 and 3), and a number of different long-chain alkanes. The main fatty acids in the biocrude (over one-third of the total peak area) are palmitic acid and palmitoleic acid. These fatty acids likely arise from hydrolysis of triacylglycerols present in the *Nannochloropsis sp.*, which is about 28% lipids. In addition to fatty acids, the crude bio-oil contained more than 10 different long-chain alkanes, such as pentadecane, heptadecane, substituted hexadecanes, nonadecane, docosane, heptacosane, nonacosane, triacontane, hentriacontane, and heptacosane. These compounds accounted for about 20% of the total peak area. The fatty acids and the long-chain alkanes in the crude bio-oil can lead to high viscosity.

Figure 4 compares total ion chromatograms of crude bio-oils produced from hydrothermal processing with no catalyst, with added Pd/C catalyst, and with both added Pd/C catalyst and added high-pressure H_2. The peak regions labeled “a” and “b” represent fatty acids and alkanes, respectively. Noncatalytic hydrothermal liquefaction produced a bio-oil that was richer in fatty acids than alkanes, judging by the relative sizes of peak regions a and b in the bottom-most chromatogram. Adding the Pd/C catalyst, which has good activity for deoxygenation of

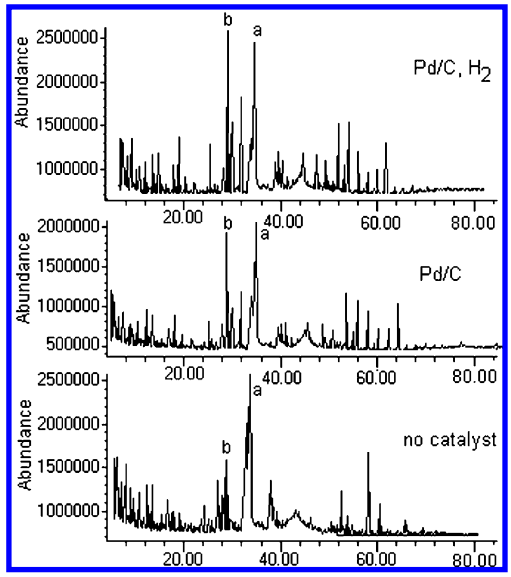

Figure 4. Total ion chromatograms of biocrude from liquefaction with and without Pd/C and H_2.

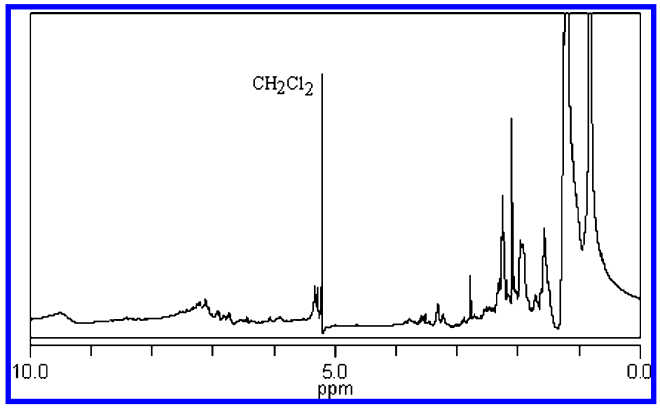

Figure 5. ^{1}H NMR spectrum of biocrude in $CDCl_3$ (Pd/C, no H_2).

fatty acids in HTW,[23] leads to a biocrude with comparable peak heights in both the alkane and the fatty acid regions (center chromatogram). Finally, adding both high-pressure H_2 and the catalyst led to alkane peak heights exceeding those of the fatty acid region (top chromatogram). These results are consistent with the Pd/C catalyst being effective for deoxygenating fatty acids as these molecules were produced during liquefaction. Converting fatty acids to alkanes improves the storage stability of the fuel and also increases its energy density.

3.3.2. NMR Analysis. ^{1}H and ^{13}C NMR spectroscopies identify the types and amounts of functional groups in the molecules in the bio-oil. The chemical shift provides information about the identity of the functional group, and the peak areas provide information about their relative abundances. We performed NMR analysis of the bio-oil obtained from liquefaction of *Nannochloropsis* with Pd/C catalyst.

Figure 5 shows the ^{1}H NMR spectrum. It contains large peaks at 0.83 and 1.21 ppm, which are characteristic of terminal methyl groups and methylene groups in alkyl chains, respectively.[24] The appearance of these strong peaks is consistent with the abundance of fatty acids and alkanes in the total ion chromatogram. The smaller peaks at about 1.5−1.6 and 2.1−2.3 ppm are consistent with resonances expected from protons on carbon atoms β and α, respectively, to an acyl group, as in a fatty acid. The peaks at 5.2−5.4 ppm are likely due to alkenyl protons. Most of the strong peaks reside within the 0.0−2.2 ppm range, where aliphatic methyl and methylene protons appear. Integrating these peaks leads to estimate of the overall aliphatic hydrogen content of least 80%. This high content of aliphatic protons is consistent with the molecular identities (e.g., fatty acids, alkanes) shown in Figure 3 for the major peaks in the total ion chromatogram. There are also some smaller peaks around 7 ppm, and these could arise from aromatic protons or conjugated dienes.

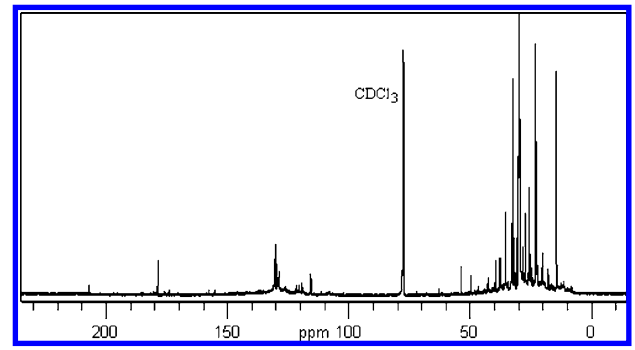

Figure 6. ^{13}C NMR of biocrude in $CDCl_3$ (Pd/C, no H_2).

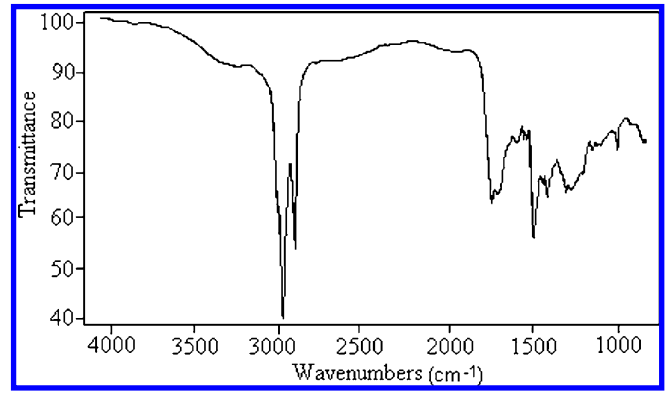

Figure 7. FT-IR spectrum of crude bio-oil (Pd/C, no H_2).

Figure 6 displays the ^{13}C NMR spectrum of the crude bio-oil. There are numerous peaks in the 10−55 ppm region, where aliphatic methyl and methylene carbon atoms appear.[25] Apart from the solvent peak, there is very little signal in the 70−100 ppm region where carbohydrate carbons appear. Recall, however, that the microalga was 12 wt % carbohydrate. This finding suggests that algal carbohydrate carbon was converted to other products in the crude bio-oil. The next peaks appear at about 115 and 130 ppm, and resonances in this region are consistent with the presence of alkenyl and aromatic carbon being present in the crude bio-oil. Finally, the peak at about 180 ppm is located in the region where one would expect to find carbon atoms in carboxylic acid groups. Of course, this peak is consistent with the presence of fatty acids in the bio-oil.

3.3.3. FT-IR Analysis. The GC−MS and NMR results indicated that the biocrude contains primarily methylene groups either in alkanes or in fatty acids. The IR results, shown in Figure 7, are consistent with this characterization. The asymmetrical and symmetrical C−H stretching vibrations in aliphatic methylene groups appear between 2840 and 3000 cm^{-1}, and two large bands are present in this region in Figure 7. The spectrum also shows strong absorbance near 1465 cm^{-1} where the scissoring band in methylene groups appears.[24] This peak might also be due to any mononuclear aromatic compounds that are present in the oil. The high intensity in these two regions is consistent with a significant amount of the hydrogen in the crude bio-oil being aliphatic. The C−O stretching band in COOH groups appears between 1650−1760 cm^{-1}, and the presence in

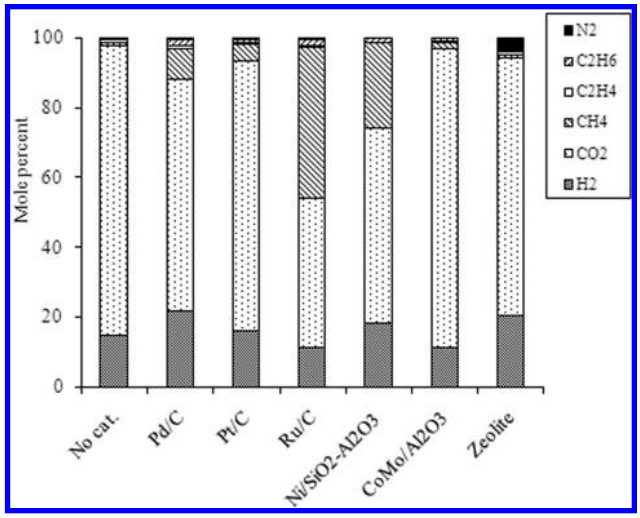

Figure 8. Influence of catalyst on gas composition (no H_2 added).

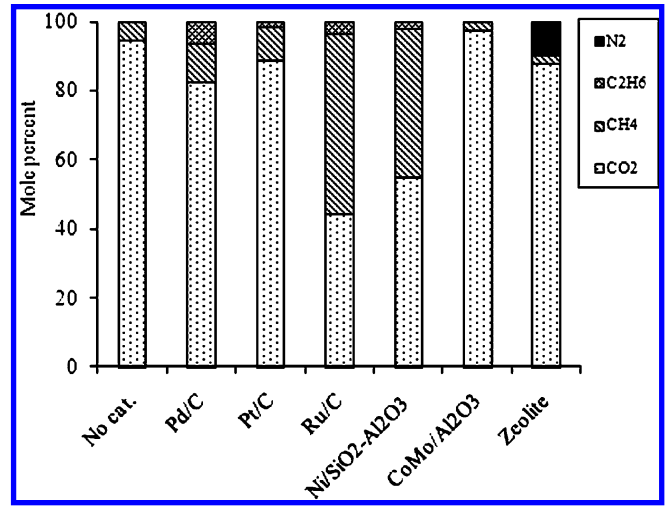

Figure 9. Influence of catalyst on gas composition (high-pressure H_2).

Figure 7 of a peak in this region is consistent with the presence of fatty acids in the crude bio-oil.

3.4. Effect of Catalysts on Gas Yields and Composition. Gases formed along with the crude bio-oil during the hydrothermal processing with and without catalysts. Figure 8 shows the gas composition from experiments done in the absence of added H_2. The main components in the gas phase are typically CO_2, H_2, and CH_4. CO_2 was typically present in the highest amount, as is common for hydrothermal processing of biomass. CO_2 can be formed from reactions such as steam re-forming and water−gas shift, which also produce hydrogen.

H_2 is present in much smaller amounts than CO_2, however,

Steam re-forming:

$$C_xH_yO_z + (2x - z)H_2O \rightarrow xCO_2 + (y/2 + 2x - z)H_2$$

Water−gas shift reaction:

$$CO + H_2O \rightarrow CO_2 + H_2$$

so much of the CO_2 must form from other reactions. The existence of separate pathways for CO_2 and H_2 formation is also supported by the disparity in their activation energies for formation from microalgae (38 ± 3 kJ/mol vs 99 ± 5 kJ/mol, respectively) during uncatalyzed hydrothermal liquefaction.[19] Methane formation could be via the methanation reaction.

$$CO + 3H_2 \rightarrow CH_4 + H_2O$$

This route seems likely, especially for the runs with Ru and Ni catalysts, which are known to give high CH_4 yields from biomass under hydrothermal conditions.[5] CO was not detected in the gas products, possibly because any CO that formed would have been consumed in the water−gas shift and methanation reactions by the end of the 60 min experiment. Our previous work on biomass gasification in supercritical water showed that the CO yields were always highest at the early stages of the reaction, and that the CO reacted away as time progressed.[25,26] It is quite likely that any CO produced had reacted away during the 60 min processing time.

It is clear from Figure 8 that the presence and type of catalyst affects the gas composition. Pd/C, $Ni/SiO_2-Al_2O_3$, and zeolite increased the mole fraction of hydrogen relative to uncatalyzed hydrothermal processing. Pd/C, Pt/C, Ru/C, and $Ni/SiO_2-Al_2O_3$ all increased the mole fraction of methane, but Ru and Ni had the biggest effects. Methane was the most abundant component in the gas phase from Ru/C catalyzed liquefaction. The N_2 mole fraction was appreciable only when the zeolite catalyst was used. The source of the N_2 is probably ammonia, which forms from hydrolysis of the amino acids produced by hydrothermal decomposition of the proteins in the microalga. The *Nannochloropsis* that we used is >50 wt % protein. Zeolites have been used as ammonia decomposition catalysts (to produce H_2 and N_2).[27] C_2H_4, C_2H_6, and N_2 were also produced but in smaller amounts that varied with the type of catalyst used.

Results from the experiments done in a high-pressure H_2 environment appear in Figure 9. The mole fractions shown are calculated on a H_2-free basis, so they reflect the relative amounts of the different gases that are solely products of hydrothermal processing. H_2 is also a potential product, but it was present at the start of the reaction so it would also be a potential reactant. The trends here with respect to methane and nitrogen are the same as those for the runs in the inert environment. Namely, Ru and Ni lead to very high methane mole fractions, and the zeolite leads to a measurable amount of N_2 formation. No ethylene was detected in the experiments with added H_2. Presumably, if it formed, it was hydrogenated to ethane.

Figure 10 shows the yields of each gas formed from microalga processing with different catalysts and reaction environments. The CO_2 yields were higher in the reducing environment with the addition of Ru and Ni. The other catalysts had less effect. The CO_2 yield with a given catalyst was generally higher in the absence rather than in the presence of H_2. These reduced CO_2 yields in the experiments with added H_2 could be due to the pressure being higher in the H_2-charged reactors rather than due to the atmosphere being reducing. The methane yields were largely insensitive to the reaction environment, being nearly the same both with and without added H_2. These yields were strongly dependent on the catalyst, however. Ru/C and the supported Ni catalyst led to high methane yields, which is consistent with the literature on hydrothermal gasification of biomass.[5]

This literature suggests that one might have anticipated higher gas yields in the present experiments. Complete gasification of biomass has been reported at similar temperatures but at higher effective catalyst loadings.[28] As noted previously, it is possible that catalyst poisoning or intraparticle diffusion limitations led to reduced gasification activity for the microalga we investigated. To determine whether poisoning by sulfur in the algae diminished the gas yields, we performed complementary experiments with palmitic acid under reaction conditions identical to those used with the microalgae. If the sulfur in the algae were

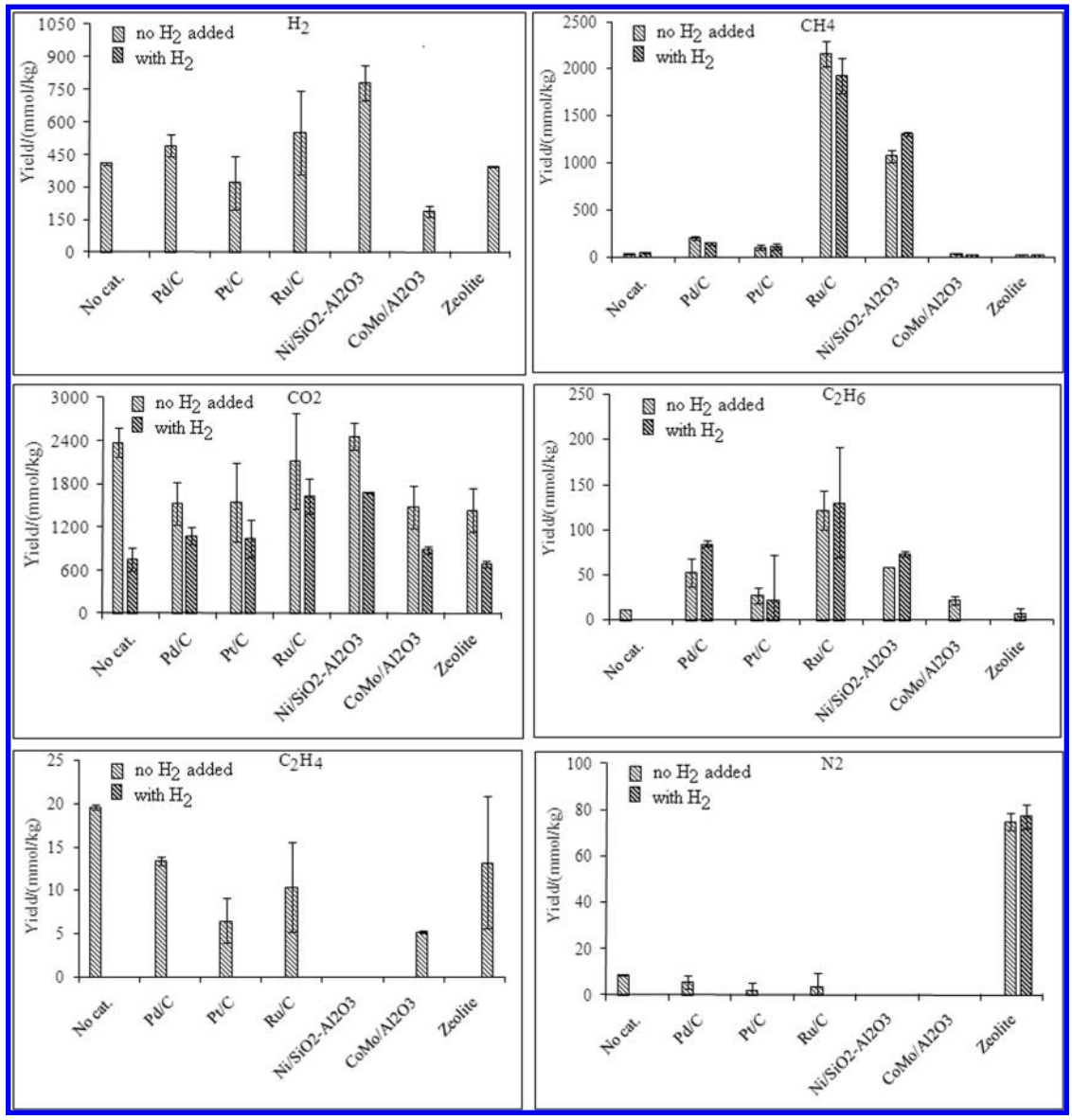

Figure 10. Gas yields from hydrothermal processing.

primarily responsible for the "low" gas yields, one would expect to observe much higher gas yields from palmitic acid, which contains no sulfur. The yields of H_2, CH_4, and C_2H_6 from palmitic acid were 335, 1885, and 120 mmol/kg with the Ru/C catalyst and 233, 58, and 33 with the Pt/C catalyst. These yields are very similar to those reported in Figure 10 for algae liquefaction with no H_2 added. Thus, it seems that sulfur poisoning is not a primary influence on the gas yields from the microalgae. Sulfur can diminish the gasification activity of the catalysts, however, as experiments with added CS_2 confirmed. When CS_2 was added to the reactor in the same proportion as S was present in the microalgae, the gas yields from palmitic acid dropped from those noted above to 133, 21, and 3.3 mmol/kg for Ru/C and 70, 15, and 7 mmol/kg for Pt/C. The methanation activity was affected most strongly, and Ru was affected much more significantly than was Pt.

The absence of any discernible difference in CH_4 yields with the addition of high-pressure H_2 was unexpected. If most CH_4 forms via methanation, then the presence of more H_2 and higher pressure should promote more methane formation, at least at equilibrium. Since no CO was detected, it is possible that under the experimental conditions used, methanation is limited by the availability of CO rather than the availability of H_2.

The yields of N_2 were also insensitive to whether H_2 was added, and the yields were low for all cases except the zeolite catalyst. The amount of nitrogen in Figure 10 for the zeolite-catalyzed run corresponds to 3.3% of the nitrogen atoms originally present in the microalgal feedstock. Thus, only a very small proportion of the nitrogen atoms are lost to N_2. As noted previously, the N_2 might be a product of ammonia decomposition, catalyzed by the zeolite.

Ru, Pd, and Ni led to the highest ethane yields. The ethane yields were strongly dependent on the catalyst identity but largely independent of the reaction environment. Conversely, the ethylene yields were strongly dependent on the reaction environment. None was detected when hydrothermal processing was done in the presence of H_2. The presence of H_2 either suppressed its formation or facilitated its conversion, perhaps to ethane, during the 60 min reaction time. In the absence of H_2, all of the catalysts produced ethylene yields that were lower than that from noncatalytic hydrothermal processing, which suggests some potential hydrogenation activity for these catalysts even in the absence of added H_2. Perhaps the H_2 generated during liquefaction served as the hydrogen source. Ethylene was not detected at all when the supported Ni catalyst was used. In this regard, it may be significant that the weight percent of active

Table 5. Atom and Energy Balances for Hydrothermal Liquefaction (No Added H_2)

catalyst	C_{oil}/C_{algae}	$(C_{oil} + C_{gas})/C_{algae}$	H_{oil}/H_{algae}	$(H_{oil} + H_{gas})/H_{algae}$	E_{oil}/E_{algae}	$(E_{oil} + E_{gas})/E_{algae}$
no cat.	0.62	0.62	0.61	0.62	0.74 ± 0.01	0.75 ± 0.01
Pd/C	0.97	0.98	1.03	1.06	1.19 ± 0.04	1.21 ± 0.05
Pt/C	0.85	0.85	0.87	0.89	1.03 ± 0.09	1.04 ± 0.09
Ru/C	0.84	0.91	0.86	1.03	1.01 ± 0.05	1.14 ± 0.05
$Ni/SiO_2-Al_2O_3$	0.88	0.92	0.86	0.96	1.05 ± 0.06	1.12 ±0.06
$CoMo/Al_2O_3$	0.95	0.95	0.93	0.94	1.13 ± 0.03	1.14 ± 0.03
zeolite	0.74	0.75	0.73	0.74	0.88 ± 0.20	0.89 ± 0.20

Table 6. Atom and Energy Balances for Hydrothermal Liquefaction in High-Pressure H_2

catalyst type	C_{oil}/C_{algae}	$(C_{oil} + C_{gas})/C_{algae}$	H_{oil}/H_{algae}	$(H_{oil} + H_{gas})/(H_{algae} + H_{2\ feed})$	E_{oil}/E_{algae}	$(E_{oil} + E_{gas})/(E_{algae}+E_{H_2\ feed})$
no cat.	0.81	0.81	0.82	1.08	0.98 ± 0.11	0.96 ± 0.08
Pd/C	0.76	0.76	0.78	1.04	0.92 ± 0.05	0.92 ± 0.04
Pt/C	0.91	0.91	0.95	1.17	1.11 ± 0.03	1.06 ± 0.02
Ru/C	0.67	0.73	0.70	1.08	0.82 ± 0.28	0.91 ± 0.21
$Ni/SiO_2-Al_2O_3$	0.72	0.76	0.73	1.06	0.87 ± 0.03	0.92 ± 0.02
$CoMo/Al_2O_3$	0.77	0.77	0.77	1.05	0.93 ± 0.20	0.93 ± 0.14
zeolite	0.70	0.70	0.71	1.01	0.84 ± 0.34	0.86 ± 0.25

metal in the nickel catalyst is much higher (65 wt %) than that of other supported catalysts (5 wt %) in this study.

3.5. Atomic and Energy Balances. Tables 5 and 6 give the ratios of carbon, hydrogen, and chemical energy (HHV) in the bio-oil product relative to those quantities in the microalgal feedstock for processing with or without added H_2, respectively. A ratio of unity denotes recovery of the same number of atoms or amount of chemical energy in the products that was originally present in the feedstock.

Liquefaction in the inert environment (Table 5) benefited from the addition of catalysts, as the carbon atom recovery in the fuel products (oil + gas) increased from 62% for noncatalytic liquefaction to greater than 90% with most of the catalysts. Likewise, the hydrogen atom ratio for the oil increased when catalysts were used. These higher C and H yields in the products led to a higher energy recovery of 90−120% for catalyzed liquefaction. Energy recoveries exceeding 100% can arise when the oil has a lower oxygen content than the feedstock. Also, hydrogen atoms from the water can be transferred to the fuel products during the hydrothermal processing. Of course, the values in Table 5 exceed 100% by only a modest amount, and this amount could also be attributed to systematic errors (e.g., in the moisture content of the algae paste feedstock, in the yield of the crude bio-oil, in the estimated heating value of the biocrude) not included in the run-to-run random variability captured by the uncertainties given in the table. Table 5 also shows that the energy content of the gas phase was significant only for the runs that used the Ru and Ni catalysts. These energy recoveries, which were about 10% higher, are due to the promotion of methane formation by these catalysts.

Liquefaction in the reducing environment (Table 6) showed little improvement in C, H, or energy recovery upon the addition of catalysts, but in fairness, it had little room to do so, as the energy recovery was 98% even in the absence of catalyst. The energy recovery (E_{oil}/E_{algae}) was generally lower for catalytic liquefaction in the reducing environment (Table 6) than in the inert environment (Table 5), but the uncertainties are large enough that we cannot make this claim unequivocally. Interestingly, a comparison of the H_{oil}/H_{algae} entries in Tables 5 and 6 shows that the ratio of H in the bio-oil to H in the dry algae feedstock was not increased by the presence of high-pressure H_2 in the reactor, except for the case of noncatalytic liquefaction and processing with the Pt/C catalyst. Thus, it appears that adding high-pressure H_2 did not guarantee more H atoms appearing in the biocrude product. Of course, the elemental analysis showed that the oils produced under the reducing environment did have a higher H content. But, since the oil yields were generally lower in the reducing environment, the total H atom recovery was also lower.

Table 6 also shows the atom and energy balances with the gaseous products included. The C and H recoveries, when gaseous products are included, are largely identical to those for the oil alone except for the runs with Ru and Ni catalysts. Again, these catalysts promoted methane formation, so the C and H recoveries are higher with these catalysts when the gas-phase products are included. The fourth column in Table 6 shows the ratio of hydrogen atoms in the oil and gas phases (including those in the unreacted H_2) to hydrogen atoms in algae and H_2 initially charged to the reactor. This ratio exceeds unity for all runs. This result is consistent with water molecules being active participants in the chemistry, and H atoms from water being incorporated into the oil and gas products.

4. Summary and Conclusions

The crude bio-oils produced from catalytic hydrothermal liquefaction contain nearly 100% of the heating value of the algal feedstock. This high energy recovery was insensitive to the identity of the catalysts tested, and for liquefaction in H_2 also insensitive to whether a catalyst was present. The bio-oils are much lower in oxygen than the original algal biomass feedstock, and their heating values are higher than those of typical petroleum heavy crudes.

The detailed molecular characterization of the crude bio-oil from Pd/C-catalyzed liquefaction represents the first such comprehensive analysis. The crude oil appeared to be similar to that generated by noncatalytic liquefaction but with a lower proportion of fatty acids and a higher proportion of alkanes. The crude bio-oil produced from catalytic hydrothermal liquefaction of the microalga studied primarily contains molecules larger than those obtained from the fast pyrolysis or liquefaction of terrestrial biomass.

Liquefaction in a high-pressure H_2 environment led to more H atoms being present in the oil plus gas products than were originally present in the alga and H_2. Incorporation of H atoms in the oil and gas from water molecules is consistent with this observation. Thus, water molecules are seemingly active participants in the liquefaction chemistry. Liquefaction in a high-pressure H_2 environment also led to crude bio-oils with an increased H content and H/C ratio. This increase, though present in nearly all experiments, was small. The main effect of high-pressure H_2 on the gas yields was to reduce the yields of CO_2

and eliminate the production of C_2H_4. The yields of methane, ethane, and N_2 were largely insensitive to whether the reaction environment was inert (He) or reducing (H_2). Moreover, the effect on the CO_2 yield could be either a pressure effect or a chemical effect.

The crude bio-oils produced from liquefaction with Pd/C, Pt/C, Ru/C, and $CoMo/Al_2O_3$ flowed easily and were much less viscous than the biocrudes from uncatalyzed or zeolite-catalyzed liquefaction. $Ni/SiO_2-Al_2O_3$ produced bio-oils that were sulfur free (or at least below detection limits). Ru/C and $CoMo/Al_2O_3$ also showed activity for desulfurization, but not to the same extent as the Ni catalyst.

The crude bio-oils produced from liquefaction with Pt/C, $Ni/SiO_2-Al_2O_3$, and $CoMo/Al_2O_3$ had lower O/C ratios than the biocrude from noncatalytic liquefaction, both in the presence and in the absence of added H_2. Moreover, the Pt/C catalyst is active for the conversion of fatty acids into alkanes.[23] Thus, catalytic hydrothermal liquefaction may be a way to produce a crude hydrocarbon bio-oil directly from wet microalgae in a single processing step.

The different catalysts had different effects on the gas yields and composition. Ni and Ru were the most effective materials for increasing H_2 yields. These two materials were also the best at producing CH_4. The zeolite catalyst was the only one to produce high yields (relative to those produced by the other catalysts) of N_2. Catalytic decomposition of NH_3 (derived from proteins in the algal biomass) is a possible path for N_2 formation.

Acknowledgment

We gratefully acknowledge financial support from the University of Michigan College of Engineering and from the U.S. National Science Foundation (EFRI-0937992).

Literature Cited

(1) Clarens, A. F.; Resurreccion, E. P.; White, M. A.; Colosi, L. M. Environmental life cycle comparison of algae to other bioenergy feedstocks. *Environ. Sci. Technol.* **2010**, *44*, 1813–1819.

(2) Goyal, H. B.; Seal, D.; Saxena, R. C. Bio-fuels from thermochemical conversion of renewable resources: A review. *Renew. Sust. Energy Rev.* **2008**, *12*, 504–517.

(3) Savage, P. E. ; Huelsman, C.; Levine, R. B. Hydrothermal processing of biomass. In *Thermochemical conversion of biomass to liquid fuels and chemicals*; Crocker, M., Ed.; RSC Publishing: Cambridge, U.K., 2010; pp 190−219.

(4) Peterson, A. A.; Vogel, F.; Lachance, R. P.; Fröling, M.; Antal, M. J., Jr.; Tester, J. W. Thermochemical biofuel production in hydrothermal media: A review of sub- and supercritical water technologies. *Energy Environ. Sci.* **2008**, *1*, 32–65.

(5) Elliott, D. C. Catalytic hydrothermal gasification of biomass. *Biofuel. Bioprod. Bior.* **2008**, *2*, 254–265.

(6) Matsumura, Y.; Minowa, T.; Potic, B.; Kersten, S. R. A.; Prins, W.; van Swaaij, W. P. M.; van de Beld, B.; Elliott, D. C.; Neuenschwander, G. G.; Kruse, A.; Antal, M. J., Jr. Biomass gasification in near- and supercritical water: Status and prospects. *Biomass Bioenerg.* **2005**, *29*, 269–292.

(7) Akiya, N.; Savage, P. E. Roles of water for chemical reactions in high-temperature water. *Chem. Rev.* **2002**, *102*, 2725–2750.

(8) Savage, P. E. Organic chemical reactions in supercritical water. *Chem. Rev.* **1999**, *99*, 603–622.

(9) Dote, Y.; Sawayama, S.; Inoue, S.; Minowa, T.; Yokoyama, S.-ya. Recovery of liquid fuel from hydrocarbon-rich microalgae by thermochemical liquefaction. *Fuel* **1994**, *74*, 1375–1378.

(10) Minowa, T.; Yokoyama, S.-ya; Kishimoto, M.; Okakura, T. Oil production from algal cells of Dunaliella tertiolecta by direct thermochemical liquefaction. *Fuel* **1995**, *74*, 1735–1738.

(11) Yang, Y. F.; Feng, C. P.; Inamori, Y.; Maekawa, T. Analysis of the energy conversion characteristics in liquefaction of algae. *Resour. Conserv. Recycl.* **2004**, *43*, 21–33.

(12) Ross, A. B.; Biller, P.; Kubacki, M. L.; Li, H.; Lea-Langton, A.; Jones, J. M. Hydrothermal processing of microalgae using alkali and organic acids. *Fuel* **2010**, *89*, 2234–2243.

(13) Zhou, D.; Zhang, L.; Zhang, S.; Fu, H.; Chen, J. Hydrothermal liquefaction of macroalgae *Enteromorpha prolifera* to bio-oil. *Energy Fuels* **2010**, *24*, 4054–4061.

(14) Jena, U.; Das, K. C. Production of biocrude oil from microalgae via thermochemical liquefaction process. 2009 Bioenergy Engineering Conference, 2009; BIO-098024

(15) Stucki, S.; Vogel, F.; Ludwig, C.; Haiduc, A. G.; Brandenberger, M. Catalytic gasification of algae in supercritical water for biofuel production and carbon capture. *Energy Environ. Sci.* **2009**, *2*, 535–541.

(16) Chakinala, A. G.; Brilman, D. W. F.; van Swaaij, W. P. M.; Kersten, S. R. A. Catalytic and non-catalytic supercritical water gasification of microalgae and glycerol. *Ind. Eng. Chem. Res.* **2010**, *49*, 1113–1122.

(17) Elliott, D. C.; Sealock, L. J., Jr.; Baker, E. G. Chemical processing in high-pressure aqueous environments. 2. Development of catalysts for gasification. *Ind. Eng. Chem. Res.* **1993**, *32*, 1542–1548.

(18) Yu, J.; Savage, P. E. Catalyst activity, stability, and transformations during oxidation in supercritical water. *Appl. Catal. B: Environ.* **2001**, *31*, 123–132.

(19) Brown, T.; Duan, P.; Savage, P. E. Hydrothermal liquefaction and gasification of microalgae Nannochloropsis sp. *Energy Fuels* **2010**, *24*, 3639–3646.

(20) Osada, M.; Hiyoshi, N.; Sato, O.; Arai, K.; Shirai, M. Effect of sulfur on catalytic gasification of lignin in supercritical water. *Energy Fuels* **2007**, *21*, 1400–1405.

(21) Miao, X.; Wu, Q.; Yang, C. Fast pyrolysis of microalgae to produce renewable fuels. *J. Anal. Appl. Pyrol.* **2004**, *71*, 855–863.

(22) Ingram, L.; Mohan, D.; Bricka, M.; Steele, P.; Strobel, D.; Crocker, D.; Mitchell, B.; Mohammad, J.; Cantrell, K., Jr. Pyrolysis of wood and bark in an auger reactor: Physical properties and chemical analysis of the produced bio-oils. *Energy Fuels* **2008**, *22*, 614–625.

(23) Fu, J.; Lu, X.; Savage, P. E. Catalytic hydrothermal deoxygenation of palmitic acid. *Energy Environ. Sci.* **2010**, *3*, 311–317.

(24) Silverstein, R. M.; Webster, F. X.; Kiemle, D. J. *Spectrometric Identification of Organic Compounds*, 7th ed.; Wiley: New York, 2005.

(25) Resende, F. L. P.; Fraley, S. A.; Berger, M. J.; Savage, P. E. Noncatalytic gasification of lignin in supercritical water. *Energy Fuels* **2008**, *22*, 1328–1334.

(26) Resende, F. L. P.; Savage, P. E. Expanded and updated results for supercritical water gasification of cellulose and lignin in metal-free reactors. *Energy Fuels* **2009**, *23*, 6213–6221.

(27) Gilles, F.; Blin, J.-L.; Toufar, H.; Briend, M.; Su, B. L. Double interactions between ammonia and a series of alkali-exchanged faujasite zeolites evidenced by FT-IR and TPD-MS techniques. *Colloids Surf. A: Physicochem. Eng. Asp.* **2004**, *241*, 245–252.

(28) Elliott, D. C.; Neuenschwander, G. G.; Hart, T. R.; Butner, R. S.; Zacher, A. H.; Engelhard, M. H.; Young, J. S.; McCready, D. E. Chemical processing in high-pressure aqueous environments. 7. Process development for catalytic gasification of wet biomass feedstocks. *Ind. Eng. Chem. Res.* **2004**, *43*, 1999–2004.

Received for review March 30, 2010
Revised manuscript received July 28, 2010
Accepted July 30, 2010

IE100758S